Modulation of the spontaneous beat-to-beat fluctuations in peripheral vascular resistance during activation of muscle metaboreflex

Masashi Ichinose, Shunsaku Koga, Naoto Fujii, Narihiko Kondo and Takeshi Nishiyasu

Am J Physiol Heart Circ Physiol 293:H416-H424, 2007. First published 16 March 2007;
doi: 10.1152/ajpheart.01196.2006

Am J Physiol Heart Circ Physiol 293: H416–H424, 2007.
First published March 16, 2007; doi:10.1152/ajpheart.01196.2006.

Modulation of the spontaneous beat-to-beat fluctuations in peripheral vascular resistance during activation of muscle metaboreflex

Masashi Ichinose,[3] Shunsaku Koga,[2] Naoto Fujii,[1] Narihiko Kondo,[3] and Takeshi Nishiyasu[1]

[1]*Institute of Health and Sport Sciences, University of Tsukuba, Tsukuba City, Ibaraki, Japan;* [2]*Applied Physiology Laboratory, Kobe Design University, Kobe, Japan; and* [3]*Faculty of Human Development, Kobe University, Kobe, Japan*

Submitted 31 October 2006; accepted in final form 12 March 2007

Ichinose M, Koga S, Fujii N, Kondo N, Nishiyasu T. Modulation of the spontaneous beat-to-beat fluctuations in peripheral vascular resistance during activation of muscle metaboreflex. *Am J Physiol Heart Circ Physiol* 293: H416–H424, 2007. First published March 16, 2007; doi:10.1152/ajpheart.01196.2006.—Continuous measurement of leg blood flow (LBF) using Doppler ultrasound with simultaneous noninvasive mean arterial blood pressure (MAP) measurement permits beat-to-beat estimates of leg vascular resistance (LVR) in humans. We tested the hypothesis that the beat-to-beat fluctuations in LVR and the dynamic relationship between MAP and LVR are modulated by the activation of muscle metaboreflex. Twelve healthy subjects performed a 1-min isometric handgrip exercise at 50% maximal voluntary contraction, which was followed by a period of imposed postexercise muscle ischemia (PEMI). We then employed transfer function analysis to examine the dynamic relationships between MAP and LBF and between MAP and LVR, both at rest (control) and during PEMI. We found the following. *1*) The spectral power for LBF and LVR in low-frequency (~0.03–0.15 Hz) range significantly increased from control during PEMI without a significant change in the high-frequency (~0.15–0.35 Hz) power. *2*) During PEMI, the transfer function gains for MAP-LBF and MAP-LVR relationships in the low-frequency (~0.05–0.15 Hz) range were significantly increased during PEMI (vs. control) but were unchanged in the high-frequency (~0.2–0.3 Hz) range. *3*) The phases for MAP-LBF and MAP-LVR relationships were not different during control and PEMI. The phase for MAP-LVR relationship revealed that changes in MAP were followed by directionally similar changes in LVR, which is consistent with the characteristics of intrinsic vascular regulatory mechanisms such as the myogenic response of the resistance arteries. We suggest that, in humans, modulation of the dynamic MAP-LVR relationship during activation of the muscle metaboreflex reflects complex interactions between intrinsic vascular regulatory mechanisms and sympathetic vascular regulation.

skeletal muscle metaboreflex; transfer function analysis; Doppler ultrasound; myogenic; arterial baroreflex

REGULATION OF PERIPHERAL VASCULAR resistance (PVR) plays a central role in the control of both arterial blood pressure and regional blood flow. Interestingly, PVR has been shown to fluctuate spontaneously, and it has been hypothesized that this spontaneous fluctuation reflects centrally mediated neurogenic vascular regulation, local vascular regulatory mechanisms, or their interaction (12, 32, 36, 43), although the actual mechanism(s) is not yet fully understood (51). Similarly, arterial blood pressure also fluctuates spontaneously over a wide range of time scales (3, 23, 33, 47, 52), and the regulation of PVR as it relates to changes in blood pressure has been studied from the perspectives of the vascular component of arterial baroreflexes and autoregulatory mechanisms (6, 18, 21, 27, 30, 32, 33, 41, 43). For example, cross-spectral analysis of data from areflexic, conscious rats revealed that, in the absence of intact feedback loops, both systemic and regional vascular conductances lagged ~1 s behind mean arterial blood pressure (MAP), which suggests that autoregulatory-like mechanisms accentuate spontaneous short-term variability in MAP (32). In contrast, in rats with intact reflexes, there was reduced coherence between MAP and vascular conductance in the low-frequency (LF) range (below ~0.1 Hz) (32), which is consistent with the poor relationship often found in humans between LF oscillation of muscle sympathetic nerve activity (MSNA) and MAP under resting conditions (15, 37, 56). Neither vascular conductance nor resistance was measured in these experiments, however. In addition, whereas it is well established that evoked changes in blood pressure activate the arterial baroreflexes causing compensatory reflex changes in MSNA (13, 22) and PVR (21, 30, 41), autoregulation that might counteract the arterial baroreflexes (6) has been shown to act within individual vascular beds, such as in the brain (4, 5, 8, 16, 20, 57, 59), kidney (19, 28, 58), and other regions (17, 27, 34, 49).

Dynamic cerebral autoregulation in humans has been studied by using a transfer function analysis of the relationships between arterial blood pressure and cerebral blood flow velocity (4, 11, 20, 42, 59) and arterial blood pressure and cerebrovascular resistance index (11, 20). Another recent study (43) examined the dynamic relationship between MAP and total PVR in humans and found that the phase relationship between MAP and total PVR is consistent with an autoregulatory system (i.e., changes in MAP were followed by directionally similar changes in total PVR), just as is observed in the cerebral circulation. However, the dynamic nature of the relationships between blood pressure and vascular resistance or blood pressure and blood flow within regional vascular beds, with the exception of the cerebral vasculature, has never been examined in humans. It is possible that, in other vascular beds, such as skeletal muscles, which are not as dependent on constant flow as is the brain, the dynamic relationships between spontaneous changes in blood pressure and vascular resistance or blood flow are not consistent with the constant flow mechanisms that govern the cerebral circulation. Instead, they may exhibit the characteristics of the vascular component of the arterial baroreflexes (21, 30, 41) or those of an intrinsic response of vascular smooth muscle to changes in blood pressure (17, 27, 31, 49, 53). Furthermore, the increase in sympathetic nerve activity (SNA) might modulate the dynamic

Address for reprint requests and other correspondence: T. Nishiyasu, Institute of Health and Sport Sciences, Univ. of Tsukuba, Tsukuba City, Ibaraki 305-8574, Japan (e-mail nisiyasu@taiiku.tsukuba.ac.jp).

The costs of publication of this article were defrayed in part by the payment of page charges. The article must therefore be hereby marked "*advertisement*" in accordance with 18 U.S.C. Section 1734 solely to indicate this fact.

blood pressure-vascular resistance and/or blood pressure-blood flow relationships. However, these have never been tested.

In the present study, we combined ultrasound Doppler measurement of leg blood flow (LBF) with continuous noninvasive measurement of MAP to explore the dynamic relationships between spontaneous changes in MAP and vascular resistance or blood flow in the leg vasculature. This was accomplished with transfer function analysis of the data collected from subjects at rest and during postexercise muscle ischemia (PEMI), which evokes a substantial increase in SNA via activation of the muscle metaboreflex (2, 21–23, 38–40, 44). We hypothesized that the dynamic relationships between MAP and leg vascular resistance (LVR) or LBF of resting humans would be characteristic of the vascular component of the arterial baroreflex rather than that of autoregulatory mechanisms and, furthermore, that sympathoexcitation by the muscle metaboreflex would modulate the dynamic MAP-LVR or MAP-LBF relationships.

METHODS

Subjects. We studied 12 healthy male volunteers with a mean age of 24 ± 1 yr, body weight of 64.7 ± 2.2 kg, and height of 172.0 ± 1.1 cm. None of the subjects was receiving medication, and none smoked. The study, which was carried out in accordance with the Declaration of Helsinki, was approved by the Human Subjects Committee of the University of Tsukuba, and each subject gave informed written consent.

Procedures. After entering the test room, which was maintained at 25°C, each subject assumed a supine position. He then performed a maximum voluntary contraction (MVC) using a handgrip dynamometer, which enabled us to determine 50% MVC. Thereafter, one rapidly inflatable cuff for arterial occlusion was placed on the upper arm (for the production of PEMI), another cuff was placed on the ankle ipsilateral to the femoral artery used for blood flow measurements (see below), and a respiratory mask was fitted. The subjects then had a rest period of at least 15 min before data collection began.

The subjects were instructed to maintain a constant rate of breathing (15 cycles/min) and a constant tidal volume of 0.4–0.7 liters throughout the experiment. We previously established that this tidal volume did not cause dyspnea at a constant respiratory frequency of 15 cycles/min in any subject. Auditory signals and an oscilloscope display of the respiratory volume were supplied to assist the subject with this. Throughout the measurement period, the occlusion cuff on the ankle was kept inflated to a supersystolic pressure (>240 mmHg) to impede the foot circulation. Because the foot has a rich skin vasculature, including arteriovenous anastomoses, which can be affected by changes in the level of arousal, circulatory arrest in the foot can minimize alterations in LVR and LBF elicited by changes in arousal level. Control data were acquired for 5 min before handgrip exercise were started. The subject then performed a 60-s isometric handgrip exercise at 50% MVC with visual feedback of the achieved force on an oscilloscope display. Five seconds before cessation of the static handgrip, the occlusion cuff on the subject's arm was inflated to supersystolic pressure (>240 mmHg). The cuff remained inflated long enough to produce a 5-min period of PEMI and was then deflated.

Measurements. R-R interval was monitored via a three-lead ECG. Beat-to-beat changes in arterial blood pressure were assessed by finger photoplethysmography (Finometer; Finapres Medical Systems). The monitoring cuff was placed around the middle finger with the forearm and hand supported so that the cuff was aligned at the level of the heart. The subject wore a mask connected to a respiratory flow meter (RF-H; Minato Medical Science) for the measurement of respiratory flow.

An ultrasound Doppler system (HDI 5000; ATL Ultrasound) equipped with a hand-held transducer probe (model L12–5) with an operating frequency of 6 MHz was utilized to simultaneously measure two-dimensional femoral artery diameter and blood velocity. All measurements were made with the transducer probe positioned over the common femoral artery, 2–3 cm distal to the inguinal ligament. All Doppler data were recorded continuously on S-VHS videotape (ST-120; Maxell). The videotape record of the vessel image was digitized with a digital video board (PCI-1411; National Instruments) and stored in a personal computer (ThinkPad T30; IBM) equipped with a computer program for measuring vessel diameter. The femoral artery diameters related to systole (D_s; mm) and to diastole (D_d; mm) were taken as the largest and smallest diameter within each cardiac cycle, respectively. The mean diameter (D_m; mm) was calculated as follows:

$$D_m = D_s/3 + 2 \cdot D_d/3 \quad (1)$$

We calculated D_m for each minute of the control and PEMI periods as the mean value of D_m from 20 consecutive beats. Because D_m did not change over time during either the control or PEMI period, we averaged 5 min of D_m to obtain one representative value for control and PEMI, respectively. The cross-sectional area of the femoral artery (CSA_{FA}; cm^2) was estimated by using the representative D_m as follows:

$$CSA_{FA} = (D_m/10/2)^2 \cdot \pi \quad (2)$$

Instantaneous mean blood velocity (MBV) was continuously estimated by means of a computer program developed with the aid of LabVIEW (version 6.0; National Instruments). The processes used in the calculation of MBV have been described in detail elsewhere (21). Briefly, the frequency spectrum of the analog audio output signal of our ultrasound Doppler unit robustly reflects the Doppler shift frequency spectrum within the audio range (<7.5 kHz in this study). The mean frequency (f_{me}) of the analog audio signal calculated by our system correlated very well with the actual mean Doppler-shift frequency when an electrically generated arbitrary ultrasound wave was transmitted to the transducer probe and measured with our ultrasound Doppler unit [$y = 0.99x - 3.21$ ($r^2 = 0.99$)] (see Fig. 2 in Ref. 22). We therefore regarded f_{me} as the mean Doppler shift frequency and used it to calculate instantaneous MBV (see below). Our system continuously produces 100 values of f_{me} per second (100 Hz). The analog signals representing the ECG, blood-pressure waveform, and respiratory flow were digitized at a sampling frequency of 100 Hz and stored together with f_{me}. This enabled all of the data to be analyzed together for the same time period. R-R intervals, systolic arterial blood pressure (SAP), diastolic arterial blood pressure (DAP), MAP, and MBV were calculated with an off-line data-analysis program. MBV was derived from the stored f_{me} data with the use of the following formula:

$$MBV = \frac{f_{me} \cdot C}{2 \cdot f_e \cdot \cos\theta} \times 100 \quad (3)$$

where f_e is the emitted frequency from the transducer probe (6 MHz in our setting), C is the sound velocity in the tissues (we employed 1,530 m/s), and θ is the angle between the blood flow direction and the ultrasound beam (we kept θ below 60°). We applied the above formula to all of the stored f_{me} data and obtained an instantaneous MBV profile over the entire measurement period. The instantaneous MBV profile was then averaged over each cardiac cycle to acquire the beat-to-beat MBV (MBV_{bb}; cm/s). LBF was derived from the following formula:

$$LBF\ (ml/min) = CSA_{FA}\ (cm^2) \times MBV_{bb}\ (cm/s) \times 60 \quad (4)$$

and LVR was calculated as follows:

$$LVR = MAP/LBF \quad (5)$$

MBV data were successfully collected from 11 of the 12 subjects, and the LBF and LVR data shown here are from those 11 subjects.

Data analysis. Of the 5-min recordings made during the control and PEMI periods, we used the 4.5-min-long records starting 30 s after the end of handgrip exercise for analysis. In the PEMI data, we performed linear regression analysis between each of the measured variables vs. time (in s) for each subject to confirm the steady state of the measured variables. We found no significant correlation between variables and time, indicating that the measured variables were under steady-state condition during PEMI. The beat-to-beat data for the R-R interval, SAP, MAP, LBF, and LVR were interpolated and resampled, thus providing 512 points of equidistant time interval data. The data were then divided into five equal overlapping segments of 256 data points, and for each segment the linear trend was removed and the Hanning window was applied. Fast-Fourier transforms were implemented in each segment and then averaged to calculate the autospectrum. The spectral resolution for these estimates was ~0.0074 Hz. The high-frequency (HF; ~0.03–0.15 Hz) and LF (~0.15–0.35 Hz) powers of all of the variables were calculated from the integration of the autospectra. We also calculated the total spectral power as the total variance minus the power of the very-low-frequency (<0.03 Hz) component. We then employed transfer function analysis to evaluate the relationship between SAP and the R-R interval and between MAP and LBF or LVR. The transfer function [H(f)] between two signals was calculated as $H(f) = S_{xy}(f)/S_{xx}(f)$, where $S_{xx}(f)$ is the autospectrum of SAP or MAP variability and $S_{xy}(f)$ is the cross-spectrum between SAP and the R-R interval or between MAP and LBF or LVR. The transfer function magnitude (gain), H(f), and phase spectrum [Φ(f)] were obtained from the real [$H_R(f)$] and imaginary [$H_I(f)$] parts of the complex function as

$$|H(f)| = [H_R(f)^2 + H_I(f)^2]^{1/2} \quad (6)$$

$$\Phi(f) = \tan^{-1}[H_I(f)/H_R(f)] \quad (7)$$

The squared coherence function [Coh(f)] was estimated as

$$Coh(f) = |S_{xy}(f)|^2/[S_{xx}(f)S_{yy}(f)] \quad (8)$$

where $S_{yy}(f)$ is the autospectrum of changes in the R-R interval or LBF or LVR. The squared coherence function reflects the fraction of the output power that can be linearly related to the input power at each frequency. Similar to a correlation coefficient, it varies from 0 and 1 and reflects the validity of the transfer function estimates.

The LF and HF transfer function gain, phase, and coherence were estimated as mean values in the frequency range of ~0.05–0.15 Hz and ~0.2–0.3 Hz, respectively. For phase value interpretation, a negative phase suggests that changes in the input variable preceded changes in the output response, whereas a positive phase suggests the reverse.

Statistical analysis. Data are presented as means ± SE. Comparisons of the variables between the control and PEMI periods were made by paired *t*-test. Statistical significance was accepted at a *P* value of <0.05.

RESULTS

Basal data. Table 1 shows the group means obtained for SAP, DAP, MAP, R-R interval, LBF, LVR, and femoral artery diameter during the control and PEMI periods. During PEMI, SAP, DAP, MAP, and LVR were all higher than during control, but the R-R interval, LBF, and femoral artery diameter did not differ from results during control.

Autospectral data. An example of the central and peripheral vascular beat-to-beat data collected from a representative subject during the control and PEMI periods is depicted in Fig. 1. The group means of the autospectral power distributions in the LF and HF regions and the total power for each variable are summarized in Fig. 2. During PEMI, the LF and total R-R interval power spectra were significantly increased from control. The HF R-R interval power also tended to increase during PEMI ($P = 0.053$) but did not reach the level of statistical significance. The LF, HF, and total power for the SAP and MAP during PEMI did not differ from control. On the other hand, the LF and total power for LBF increased during PEMI, compared with control, whereas the HF LBF power was not significantly changed. Similarly, the LF and total power for LVR increased during PEMI, but the HF power did not significantly differ from control.

Table 1. *Baseline values of arterial blood pressure, R-R interval, LBF, LVR, and femoral artery diameter during the control and PEMI periods*

	Control	PEMI
SAP, mmHg	123±3.4	142±3.6*
DAP, mmHg	62±1.2	74±2.0*
MAP, mmHg	82±1.8	97±2.3*
R-R interval, ms	1022±48	990±50
LBF, ml/min	381.4±34.2	388.7±37.4
LVR, mmHg·ml^{-1}·min	0.24±0.03	0.29±0.03*
Femoral artery diameter, mm	9.7±0.1	9.8±0.1

Values are means ± SE; *n* = no. of subjects. SAP, systolic arterial pressure (*n* = 12); DAP, diastolic arterial pressure (*n* = 12); MAP, mean arterial pressure (*n* = 12); LBF, leg blood flow (*n* = 11); LVR, leg vascular resistance (*n* = 11); PEMI, postexercise muscle ischemia. *$P < 0.05$ vs. control.

Cross-spectral data relating SAP and the R-R interval. Figure 3 shows the group means of the transfer function gain, phase, and coherence for the relationship between SAP and the R-R interval; the transfer function for gain, phase, and coherence in the LF and HF ranges are summarized in Table 2. During PEMI, the transfer function gain in both the HF and LF ranges was significantly increased from that shown during control. The phase of the SAP-RR-interval relation in the LF range was negative and was unchanged from control during PEMI. On the other hand, the phase in the HF range approached 0°, although the mean value became positive and during PEMI was unchanged from control. The coherence was above 0.5 in both the LF and HF ranges during both the control and PEMI periods. In addition, although the coherence in the LF range was significantly increased during PEMI from that shown during control, coherence in the HF range was unchanged from control.

Cross-spectral data relating MAP and LBF. Figure 4 shows the group means of the transfer function gain, phase, and coherence for the relationship between MAP and LBF; the transfer function gain, phase, and coherence in the LF and HF ranges are summarized in Table 3. During PEMI, the transfer function gain in the LF range was increased from control, whereas the gain in the HF range was unchanged from control. The phase of the MAP-LBF relation in the LF range was positive during PEMI and was unchanged from that shown during control. The phase in the HF range approached 0°, and the mean values during both the control and PEMI periods were positive and did not significantly differ. The coherence was above 0.5 in both the LF and HF ranges during both the control and PEMI periods. During PEMI, coherence in the LF range was significantly increased from control, but coherence in the HF range was unchanged from control.

Cross-spectral data relating MAP and LVR. Figure 5 shows the group means of the transfer function gain, phase, and

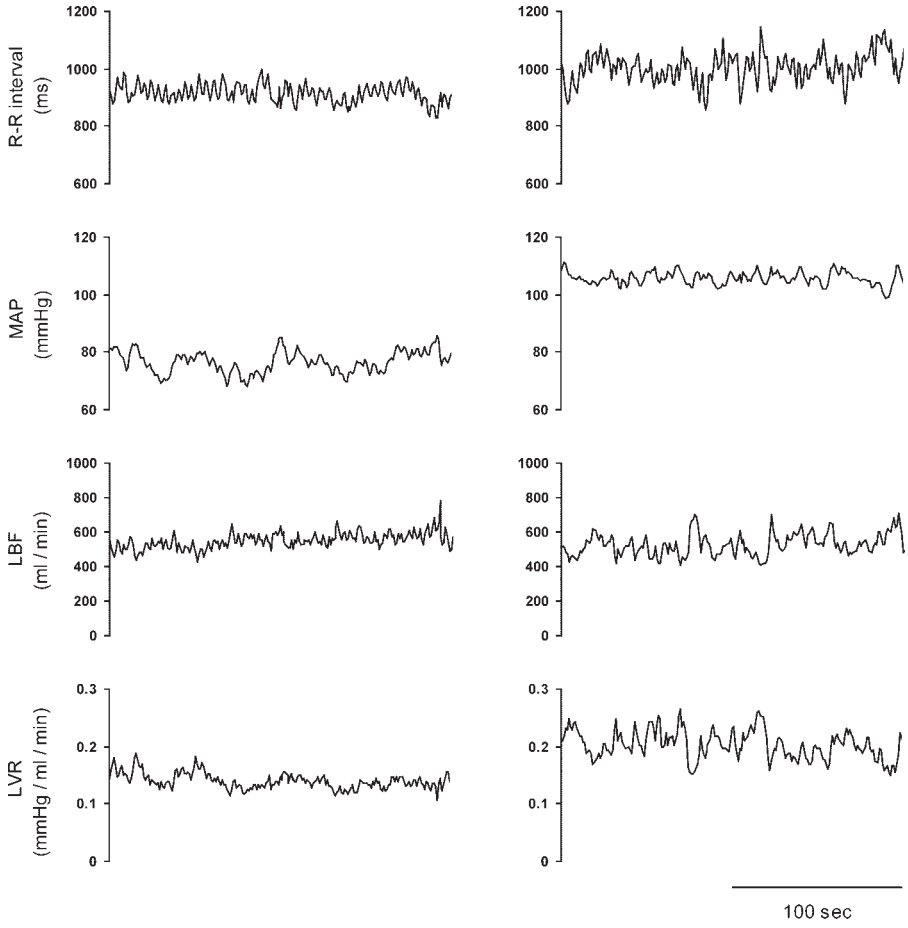

Fig. 1. Time series data from a representative subject recorded under control conditions (*left*) and during postexercise muscle ischemia (PEMI; *right*). MAP, mean arterial blood pressure; LBF, leg blood flow; LVR, leg vascular resistance.

coherence for the relationship between MAP and LVR; the transfer function gain, phase, and coherence in the LF and HF ranges are summarized in Table 4. During PEMI, transfer function gain in the LF range was increased from control, whereas the gain in the HF range was unchanged from control. The phase of the MAP-LVR relationship in the LF range was negative and did not differ in the control and PEMI periods. The phase in the HF range approached 0° during both the control and PEMI periods, although the mean value was negative. The phase in the HF range also did not differ during the control and PEMI periods. The coherence was above 0.5 in both the LF and HF ranges during both the control and PEMI periods. Coherence in the LF range was significantly increased from control during the PEMI period, but coherence in the HF range was unchanged from control.

DISCUSSION

To the best of our knowledge, this is the first study in which the spontaneous variability in LBF and LVR was quantified, and the dynamic relationships between MAP and LBF or LVR was investigated in humans. We found that the phase for the MAP-LVR relationship was negative (Table 4) and that there was a linear decrease in the phase value between ~0.03 and ~0.2 Hz in both the control and PEMI periods (Fig. 5). This pattern is consistent with a mechanism in which a change in MAP was followed, after a delay of ~1.5 s, by a directionally similar change in LVR across this range of input-to-output frequencies. This MAP-LVR relationship, which was seen under relatively steady-state conditions, appears to be separate from arterial baroreceptor detection of changes in blood pressure, such as changes in MSNA (13, 22) and PVR (21, 30, 41) evoked by neck pressure or suction, which are directionally opposite to the changes in loading state of the baroreceptors (i.e., changes in blood pressure). The progressive linear decrease in the phase with LVR after MAP in the LF range means that a matching change in MAP by a directionally opposite change in LVR could be accomplished only through a variable delay, which is also inconsistent with the known physiology of the arterial baroreflexes (33). By contrast, the phases for the MAP-LVR and MAP-LBF relationships were similar to the blood pressure-vascular resistance or blood pressure-blood flow relationships observed in vascular beds that exhibit autoregulation, such as the cerebral (4, 11, 20, 42, 59) and renal (19, 28, 58) circulations. The observed phase lead of blood flow before pressure in leg vasculature might be a simple mathematical consequence of natural phase lag of vascular resistance responding to changes in pressure by the mechanisms of autoregulation as suggested in cerebral vasculature (11). In addition, the phase for the MAP-LVR relationship, especially in the LF range, resembled the previously reported phase relationship between MAP and total PVR in humans (43).

The properties of the gain in the MAP-LBF relationship were also similar to those for the pressure-flow relationship in the cerebral (4, 11, 42, 59) and renal (19, 28) circulations. By

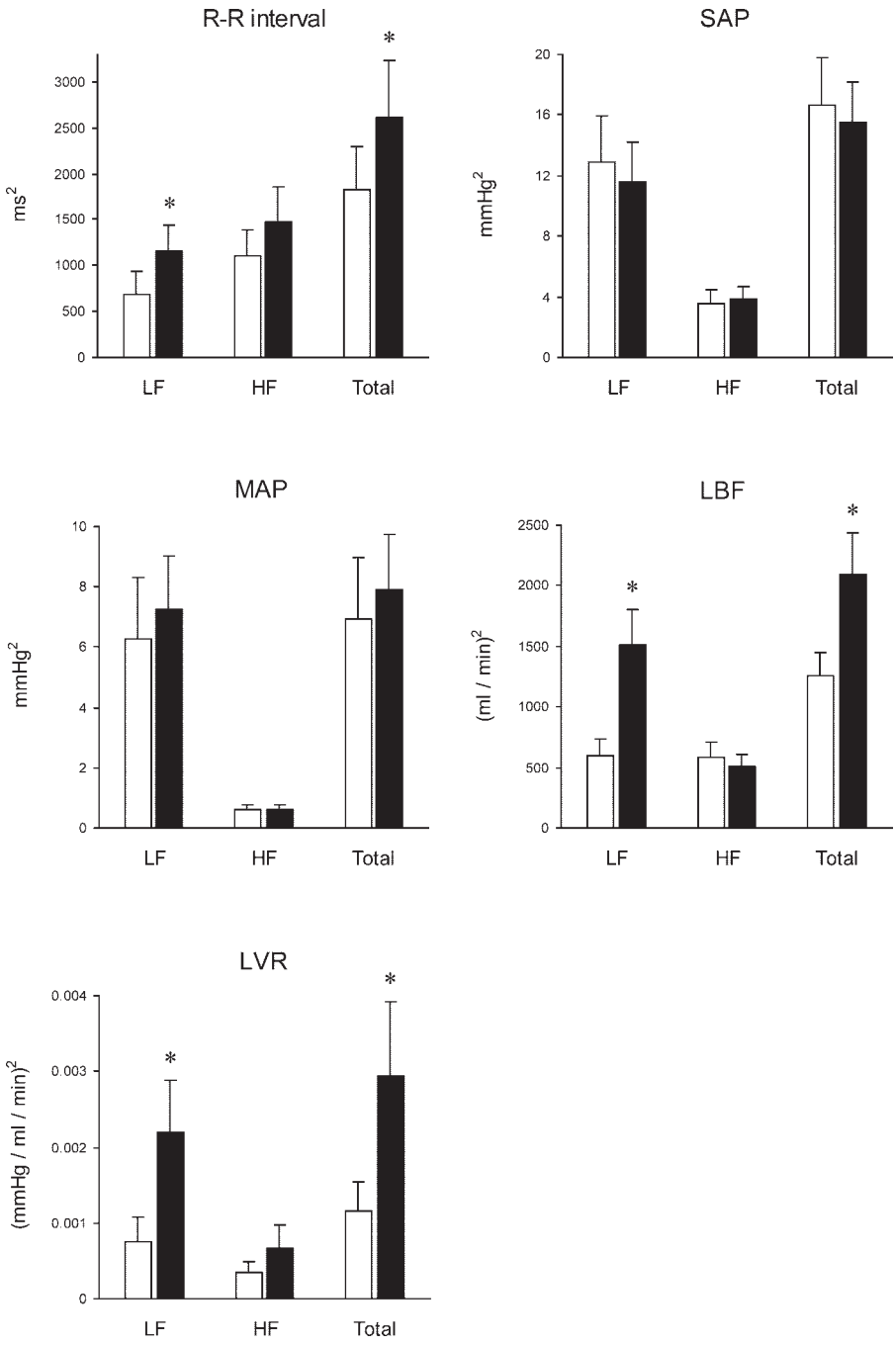

Fig. 2. Spectral power in low- (LF) and high-frequency (HF) ranges and total spectral power (Total) for the R-R interval (n = 12 subjects), systolic arterial pressure (SAP; n = 12 subjects), MAP (n = 12 subjects), LBF (n = 11 subjects), and LVR (n = 11 subjects) under control (open bars) and PEMI (solid bars) conditions. *$P < 0.05$ vs. control.

contrast, the properties of gain in the MAP-LVR relationship, i.e., low in the LF range and increasing at higher frequencies (Fig. 5, Table 4), apparently differed from those in the pressure-vascular resistance relationship in the cerebral (11, 20) and renal (19) circulations, where the gain is high in the LF range and declines at higher frequencies. On the other hand, the properties of the gain in the MAP-LVR relationship were consistent with the greater amplitude of the myogenic response seen with fast rates of rise in blood pressure in the skeletal muscle vascular beds of sympathectomized cats (17). Furthermore, in humans, the properties of the gain in the MAP-LVR relationship are quite consistent with those in the MAP-total PVR relationship (43). These observations reveal that the dynamic MAP-LVR relationship is consistent with characteristics of intrinsic vascular regulatory mechanisms, such as the myogenic response of the resistance arteries, rather than the vascular component of arterial baroreflexes.

It is difficult to provide a definitive explanation of the mechanism(s) responsible for the increase in the transfer function gain and coherence for the MAP-LVR and MAP-LBF relationships in the LF range during PEMI. Previous studies showed that, in humans, the sensitivity of the arterial baroreflex control of MSNA, leg vascular conductance, and MAP are elevated during PEMI (7, 21–23, 29). Modulation of sympathetic vascular regulation mediated by arterial baroreflexes might act to enhance LVR responses to changes in MAP during

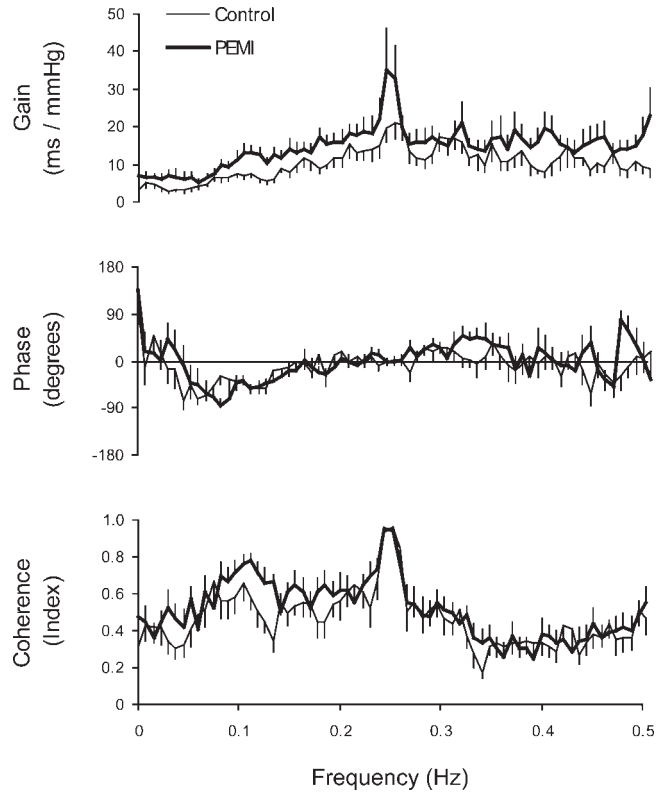

Fig. 3. Group means (±SE) for the transfer function gain (*top*), phase (*middle*), and coherence (*bottom*) for the SAP-R-R interval relationship under control and PEMI conditions (n = 12 subjects).

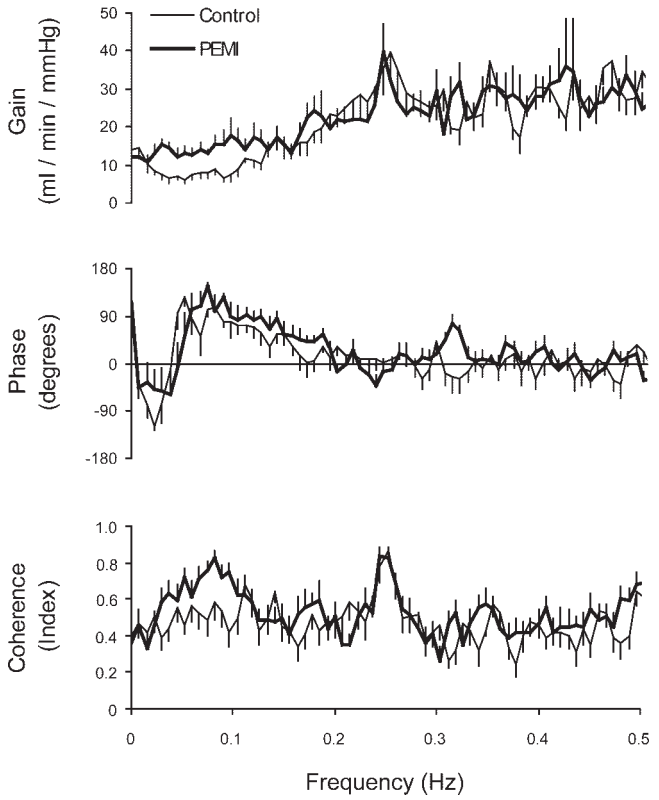

Fig. 4. Group means (±SE) for the transfer function gain (*top*), phase (*middle*), and coherence (*bottom*) for the MAP-LBF relationship under control and PEMI conditions (n = 11 subjects).

PEMI; however, as mentioned above, the relationship between spontaneous changes in MAP and LVR is inconsistent with the vascular component of arterial baroreflexes. On the other hand, in animals, it has been shown that the myogenic responses of skeletal muscle arterioles are enhanced during periods of high SNA (34, 48, 49). On the basis of those reports, it seems plausible that the augmented transfer function gain for the MAP-LVR relationship in the LF range during the PEMI period reflected the facilitation of myogenic responses of arterioles within leg muscles induced by increased SNA associated with activation of the muscle metaboreflex. This notion is also consistent with the phase relationship between the MAP and LVR in the LF range. In that case, MAP was followed by directionally similar changes in LVR after a delay of a few seconds, which likely reflects the myogenic response in skeletal muscle vascular bed (17). The precise mechanisms remain to be elucidated, however.

Although there are still arguments over interpretation (10, 35, 54), under carefully controlled experimental conditions, changes in the variability of the R-R interval likely track changes in autonomic neural control of the heart with reasonable accuracy (1, 14, 45). That the increase in the LF power of the R-R interval variability occurred simultaneously with the tendency to increase the HF power (P = 0.053) (Fig. 2) during PEMI suggests that there are simultaneous increases in cardiac sympathetic and parasympathetic tone during PEMI, confirming earlier results in both dogs (44) and humans (38). Nishi-

Table 2. *Transfer function gain and phase and coherence for the SAP-R-R interval relationship during the control and PEMI periods*

	Control	PEMI
Gain, ms/mmHg		
LF	6±0.5	10±1.2*
HF	15±2.4	20±3.8*
Phase, degrees		
LF	−41.1±6.8	−48.8±6.4
HF	6.1±5.2	9.9±5.1
Coherence		
LF	0.53±0.05	0.64±0.03*
HF	0.64±0.04	0.65±0.05

Values are means ± SE; n = 12 subjects. LF, low-frequency range; HF, high-frequency range. *P < 0.05 vs. control.

Table 3. *Transfer function gain and phase and coherence for the MAP-LBF relationship during the control and PEMI periods*

	Control	PEMI
Gain, ml·min^{-1}·mmHg^{-1}		
LF	10±1.2	15±1.9*
HF	29±2.9	26±2.6
Phase, degrees		
LF	74.5±11.0	91.6±6.3
HF	9.1±5.6	1.2±7.8
Coherence		
LF	0.52±0.04	0.63±0.03*
HF	0.56±0.06	0.53±0.04

Values are means ± SE; n = 11 subjects. *P < 0.05 vs. control.

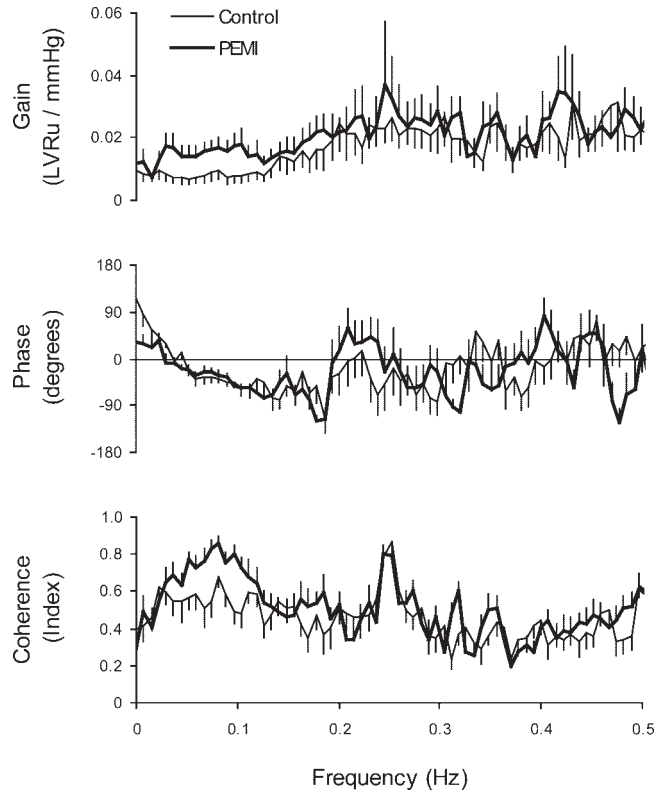

Fig. 5. Group means (±SE) for the transfer function gain (*top*), phase (*middle*), and coherence (*bottom*) for the MAP-LVR relationship under control and PEMI situations (n = 11 subjects). LVRu, leg vascular resistance units (mmHg·ml^{-1}·min).

yasu et al. (38) suggested that, in humans, such an increase in cardiac parasympathetic tone during PEMI might in part reflect the response of the arterial baroreflexes to the increase in blood pressure induced by the muscle metaboreflex.

Transfer function analysis of spontaneous variations in blood pressure and the R-R interval has been previously used to evaluate the dynamic properties of the cardiac component of arterial baroreflexes (26, 46, 50, 52). The assessment of arterial baroreflex function in this analysis reflects a closed-loop relationship between blood pressure and the R-R interval, with the basic premise that oscillation in blood pressure leads to baroreflex-mediated oscillation in the R-R interval. However, we found that, during both the control and PEMI periods, the phase in the HF range was positive, indicating that changes in the R-R interval were followed by directionally similar changes in SAP (Fig. 3, Table 2). Our results confirm a previous report (55) and suggested that respiratory sinus arrhythmia (main component of HF oscillation of R-R interval) would contribute to blood pressure fluctuations, rather than representing arterial baroreflex buffering of respiration-induced blood pressure fluctuations. Thus the increase in gain for the SAP-R-R interval relationship in the HF range observed during PEMI may reflect increased respiratory sinus arrhythmia with no change in SAP oscillations, rather than increased arterial baroreflex sensitivity.

The phase in the LF range was negative during both the control and PEMI periods (Fig. 3, Table 2), which is consistent with the cardiac baroreflexes. The increased gain in the LF range suggests that the sensitivity of the arterial baroreflex control of the cardiac interval to spontaneous changes in blood pressure in the LF range was increased during PEMI. Furthermore, the increased coherence in the LF range might also be indicative of the more dominant role played by the arterial baroreflexes in control of the cardiac interval in the LF range during PEMI than during the control period. Our results appear to be inconsistent with those of earlier reports that dynamic baroreflex control of heart rate examined by the neck chamber technique (21, 22) and the sequence technique (24) is unchanged during PEMI. These discrepancies might be attributable to differences in the autonomic nervous components that mediate cardiac baroreflex responses induced by each method. Transfer function analysis emphasizes the frequency dependence of arterial baroreflex control of the cardiac period (26, 46, 52), i.e., estimates of the transfer function in the HF range are thought to be predominantly determined by cardiac parasympathetic activity, whereas, in the LF range, they might be influenced by both cardiac sympathetic and parasympathetic activity. On the other hand, baroreflex control of heart rate examined by neck chamber and sequence techniques predominantly reflects the parasympathetic component of cardiac baroreflex (3, 9, 25, 47). We therefore believe that our results represent the first experimental indication that, in humans, the muscle metaboreflex augments the sensitivity of the cardiac arterial baroreflexes mediated by both sympathetic and parasympathetic activity.

Limitations. Cross-spectral analysis provides insight into the linear interrelationship between two variables; it does not evaluate causality. Consequently, any interpretation of relationships must be made with caution. Transfer function estimates are limited by a fundamental assumption of linearity between changes in two variables and are reliable only if squared coherence values are near or above 0.5 (11, 20, 42, 43, 50, 52). In the present study, the coherence for the SAP-R-R interval, MAP-LBF, and MAP-LVR relationships was sufficiently high in both the LF and HF ranges to confirm the validity of using this technique to assess the gain and phase for those three relationships. Transfer function analysis for the MAP-LVR relationship did not reveal feedback regulation of vascular resistance mediated by the arterial baroreflexes. Instead, the dynamic relationships between MAP and LVR or LBF were consistent with some characteristics of intrinsic vascular regulatory mechanisms, although other mechanisms cannot be ruled out. It is noteworthy that we did not induce

Table 4. *Transfer function gain and phase and coherence for the MAP-LVR relationship during the control and PEMI periods*

	Control	PEMI
Gain, LVRu/mmHg		
LF	0.009±0.002	0.015±0.003*
HF	0.022±0.005	0.027±0.008
Phase, degrees		
LF	−47.5±7.0	−44.3±6.5
HF	−38.5±23.9	−2.1±20.1
Coherence		
LF	0.54±0.04	0.68±0.02*
HF	0.53±0.05	0.52±0.04

Values are means ± SE; n = 11 subjects. LVRu, leg vascular resistance units (mmHg·ml^{-1}·min). *$P < 0.05$ vs. control.

large changes in blood pressure, such as those achieved by neck chamber stimuli, which would be expected to activate the vascular component of the arterial baroreflex (13, 21, 22, 30, 41). We therefore cannot exclude the possibility that the relationship between MAP and LVR under conditions in which there would be a greater fluctuation of blood pressure would differ from the MAP-LVR relationship observed in present study. Nonetheless, our results provide important information on the fundamental nature of the relationships between blood pressure and LVR or LBF under relatively steady-state conditions.

In summary, our results show that the dynamic responses of the R-R interval, LBF, and LVR to spontaneous changes in arterial blood pressure, as evaluated by transfer function analysis, are all augmented during PEMI-induced activation of the muscle metaboreflex. The dynamic relationship between MAP and LVR is consistent with the characteristics of intrinsic vascular regulatory mechanisms, such as the myogenic response of the resistance arteries, rather than the vascular component of arterial baroreflexes. We suggest that, in humans, modulation of the dynamic relationship between MAP and LVR during activation of muscle metaboreflex reflects complex interactions between intrinsic vascular regulatory mechanisms and sympathetic vascular regulation.

ACKNOWLEDGMENTS

We sincerely thank the volunteer subjects.

GRANTS

This study was supported by grants from Center of Excellence (COE) projects and the Ministry of Education, Science, and Culture of Japan. M. Ichinose was the recipient of a research fellowship for young scientists from Japan Society of the Promotion of Science.

REFERENCES

1. **Akselrod S, Gordon D, Ubel FA, Shannon DC, Barger AC, Cohen RJ.** Power spectrum analysis of heart rate fluctuation: a quantitative probe of beat-to-beat cardiovascular control. *Science* 213: 220–222, 1981.
2. **Alam M, Smirk FH.** Observation in man upon a blood pressure raising reflex arising from the voluntary muscles. *J Physiol* 89: 372–383, 1937.
3. **Bertinieri G, Rienzo MD, Cavallazzi A, Ferrari AU, Pedotti A, Mancia AG.** Evaluation of baroreceptor reflex by blood pressure monitoring in unanesthetized cats. *Am J Physiol Heart Circ Physiol* 254: H377–H383, 1988.
4. **Blaber PA, Bonder RL, Stein F, Dunphy PT, Moradshai P, Kassam MS, Freeman R.** Transfer function analysis of cerebral autoregulation dynamics in autonomic failure patients. *Stroke* 28: 1686–1692, 1997.
5. **Brich AA, Dinhuber MJ, Hartley-Davies R, Iannotti F, Neil-Dwyer G.** Assessment of autoregulation by means of periodic changes in blood pressure. *Stroke* 26: 834–837, 1995.
6. **Burattini R, Borgdorff P, Gross DR, Baiocco B, Westerhof N.** Systemic autoregulation counteracts the carotid baroreflex. *IEEE Trans Biomed Eng* 38: 48–56, 1991.
7. **Cui J, Wilson TE, Shibasaki M, Hodges NA, Crandall CG.** Baroreflex modulation of muscle sympathetic nerve activity during posthandgrip muscle ischemia in humans. *J Appl Physiol* 91: 1679–1686, 2001.
8. **Diehl RR, Linden D, Lücke D, Berlit P.** Phase relationship between cerebral blood flow velocity and blood pressure. A clinical test of autoregulation. *Stroke* 26: 1801–1804, 1995.
9. **Eckberg DL.** Nonlinearities of the human carotid baroreceptor-cardiac reflex. *Circ Res* 47: 208–216, 1980.
10. **Eckberg DL.** Sympathovagal balance: a critical appraisal. *Circulation* 96: 3224–3232, 1997.
11. **Edwards MR, Shoemaker JK, Hughson RL.** Dynamic modulation of cerebrovascular resistance as an index of autoregulation under tilt and controlled end-tidal CO_2. *Am J Physiol Regul Integr Comp Physiol* 283: R653–R662, 2002.
12. **Evans JM, Ziegler MG, Patwardhan AR, Ott JB, Kim CS, Leonelli FM, Knapp CF.** Gender difference in autonomic cardiovascular regulation: spectral, hormonal, and hemodynamic indexes. *J Appl Physiol* 91: 2611–2618, 2001.
13. **Fadel PJ, Ogoh S, Watenpaugh DE, Wasmund W, Olivencia-Yurvati A, Smith ML, Raven PB.** Carotid baroreflex regulation of sympathetic nerve activity during dynamic exercise in humans. *Am J Physiol Heart Circ Physiol* 280: H1383–H1390, 2001.
14. **Fouad FM, Tarazi RC, Ferrario CM, Fighaly S, Alicandri C.** Assessment of parasympathetic control of heart rate by a noninvasive method. *Am J Physiol Heart Circ Physiol* 246: H838–H842, 1984.
15. **Furlan R, Porta A, Costa F, Tank J, Baker L, Schiavi R, Rodertson D, Malliani A, Mosqueda-Garcia R.** Oscillatory patterns in sympathetic neural discharge and cardiovascular variables during orthostatic stimulus. *Circulation* 101: 886–892, 2000.
16. **Giller CA.** The frequency-dependent behavior of cerebral autoregulation. *Neurosurgery* 27: 362–368, 1990.
17. **Grände PO.** Dynamic and static components in the myogenic control of vascular tone in cat skeletal muscle. *Acta Physiol Scand Suppl* 476: 1–46, 1979.
18. **Guyton AC, Granger HJ, Coleman TG.** Autoregulation of the total systemic circulation and its relation to control of cardiac output and arterial pressure. *Circ Res* 28, *Suppl* 1: 93–97, 1971.
19. **Holstein-Rathlou NH, Wagner AJ, Marsh DJ.** Tubuloglomerular feedback dynamics and renal blood flow autoregulation in rats. *Am J Physiol Renal Fluid Electrolyte Physiol* 260: F53–F68, 1991.
20. **Hughson RL, Edwards MR, O'Leary DD, Shoemaker JK.** Critical analysis of cerebrovascular autoregulation during repeated head-up tilt. *Stroke* 32: 2403–2408, 2001.
21. **Ichinose M, Nishiyasu T.** Muscle metaboreflex modulates the arterial baroreflex dynamic effects on peripheral vascular conductance in humans. *Am J Physiol Heart Circ Physiol* 288: H1532–H1538, 2005.
22. **Ichinose M, Saito M, Wada H, Kitano A, Kondo N, Nishiyasu T.** Modulation of arterial baroreflex dynamic response during muscle metaboreflex activation in humans. *J Physiol* 544: 939–948, 2002.
23. **Ichinose M, Saito M, Wada H, Kitano A, Kondo N, Nishiyasu T.** Modulation of arterial baroreflex control of muscle sympathetic nerve activity by muscle metaboreflex in humans. *Am J Physiol Heart Circ Physiol* 286: H701–H707, 2004.
24. **Iellamo F, Pizzinelli P, Massaro M, Raimondi G, Peruzzi G, Legramante JM.** Muscle metaboreflex contribution to sinus node regulation during static exercise: insight from spectral analysis of heart rate variability. *Circulation* 100: 27–32, 1999.
25. **Iida R, Hirayanagi K, Iwasaki K, Ogawa S, Suzuki H, Yajima K.** Non-invasive assessment of human baroreflex during different body positions. *J Auton Nerv Syst* 75: 164–170, 1999.
26. **Iwasaki K, Zhang R, Zuckerman JH, Pawelczyk JA, Levine BD.** Effect of head-down-tilt bed rest and hypovolemia on dynamic regulation of heart rate and blood pressure. *Am J Physiol Regul Integr Comp Physiol* 279: R2189–R2199, 2000.
27. **Johnson PC.** Autoregulation of blood flow. *Circ Res* 59: 483–495, 1986.
28. **Just A, Wittmann U, Ehmke H, Kirchheim HR.** Autoregulation of renal blood flow in the conscious dog and the contribution of the tubuloglomerular feedback. *J Physiol* 506: 275–290, 1998.
29. **Kamiya A, Michikami D, Fu Q, Niimi Y, Iwase S, Mano T, Suzumura A.** Static handgrip exercise modifies arterial baroreflex control of vascular sympathetic outflow in humans. *Am J Physiol Regul Integr Comp Physiol* 281: R1134–R1139, 2001.
30. **Keller DM, Wasmund WL, Wray DW, Ogoh S, Fadel PJ, Smith ML, Raven PB.** Carotid baroreflex control of leg vascular conductance at rest and during exercise. *J Appl Physiol* 94: 542–548, 2003.
31. **Kitano A, Shoemaker JK, Ichinose M, Wada H, Nishiyasu T.** Comparisons of cardiovascular responses between lower body negative pressure and head-up tilt. *J Appl Physiol* 98: 2081–2086, 2005.
32. **Létienne R, Barrès C, Cerutti C, Julien C.** Short-term haemodynamic variability in the conscious areflexic rat. *J Physiol* 506: 263–274, 1998.
33. **Malpas SC.** Neural influences on cardiovascular variability: possibilities and pitfalls. *Am J Physiol Heart Circ Physiol* 282: H6–H20, 2002.
34. **Meininger GA, Faber JE.** Adrenergic facilitation of myogenic response in skeletal muscle arterioles. *Am J Physiol Heart Circ Physiol* 260: H1424–H1432, 1991.
35. **Montano N, Ruscone TG, Porta A, Lombardi F, Pagani M, Malliani A.** Power spectrum analysis of heart rate variability to assess the changes

in sympathovagal balance during graded orthostatic tilt. *Circulation* 1994: 1826–1831, 1994.
36. **Mukkamala R, Toska K, Cohen RJ.** Noninvasive identification total peripheral resistance baroreflex. *Am J Physiol Heart Circ Physiol* 284: H947–H959, 2003.
37. **Myers CW, Cohen MA, Eckberg DL, Taylor JA.** A model for the genesis of arterial pressure Mayer waves from heart rate and sympathetic activity. *Auton Neurosci* 91: 62–75, 2001.
38. **Nishiyasu T, Tan N, Morimoto K, Nishiyasu M, Yamaguchi Y, Murakami N.** Enhancement of parasympathetic cardiac activity during activation of muscle metaboreflex in humans. *J Appl Physiol* 77: 2778–2783, 1994.
39. **Nishiyasu T, Tan N, Morimoto K, Sone R, Murakami N.** Cardiovascular and humoral responses to sustained muscle metaboreflex activation in humans. *J Appl Physiol* 84: 116–122, 1998.
40. **Nishiyasu T, Ueno H, Nishiyasu M, Tan N, Morimoto K, Morimoto A, Deguchi T, Murakami N.** Relationship between mean arterial pressure and muscle cell pH during forearm ischemia after sustained handgrip. *Acta Physiol Scand* 151: 143–148, 1994.
41. **Ogoh S, Fadel PJ, Wasmund WL, Raven PB.** Haemodynamic changes during neck pressure and suction in seated and supine positions. *J Physiol* 540: 707–716, 2002.
42. **Ogoh S, Fadel PJ, Zhang R, Selmer C, Jans Ø, Sdcher NH, Raven PB.** Middle cerebral artery flow velocity and pulse pressure during dynamic exercise in humans. *Am J Physiol Heart Circ Physiol* 288: H1526–H1531, 2005.
43. **O'Leary DD, Shoemaker JK, Edwards MR, Hughson RL.** Spontaneous beat-by-beat fluctuations of total peripheral and cerebrovascular resistance in response to tilt. *Am J Physiol Regul Integr Comp Physiol* 287: R670–R679, 2004.
44. **O'Leary DS.** Autonomic mechanisms of muscle metaboreflex control of heart rate. *J Appl Physiol* 74: 1748–1754.
45. **Pagani M, Lombardi F, Guzzetti S, Rimoldi O, Furlan R, Pizzinelli P, Sandrone G, Malfatto G, Dell'Orto S, Malliani A.** Power spectral analysis of heart rate and arterial pressure variabilities as a maker of sympatho-vagal interaction in man and conscious dog. *Circ Res* 59: 178–193, 1986.
46. **Pagani M, Somers V, Furlan R, Dell'Orto S, Conway J, Baselli G, Cerutti S, Sleight P, Malliani A.** Changes in autonomic regulation induced by physical training in mild hypertension. *Hypertension* 12: 600–610, 1988.
47. **Parati G, Rienzo MD, Bertinieri G, Pomidossi G, Casadei R, Groppelli A, Pedotti A, Zanchetti A, Mancia G.** Evaluation of the baroreceptor-heart rate reflex by 24-hour intra arterial blood pressure monitoring in humans. *Hypertension* 12: 214–222, 1988.
48. **Ping P, Johnson PC.** Mechanism of enhanced myogenic response in arterioles during sympathetic nerve stimulation. *Am J Physiol Heart Circ Physiol* 263: H1185–H1189, 1992.
49. **Ping P, Johnson PC.** Role of myogenic response in enhancing autoregulation of flow during sympathetic nerve stimulation. *Am J Physiol Heart Circ Physiol* 263: H1177–H1184, 1992.
50. **Robbe HWJ, Mulder LJM, Ruddek H, Langewitz WA, Veldman JBP, Mulder G.** Assessment of baroreceptor reflex sensitivity by means of spectral analysis. *Hypertension* 10: 538–543, 1987.
51. **Rowell LB.** *Human Circulation.* New York: Oxford Univ Press, 1986, p. 8–43.
52. **Saul JP, Berger RD, Albrecht P, Stein SP, Chen MH, Cohen RJ.** Transfer function analysis of the circulation: unique insight into cardiovascular regulation. *Am J Physiol Heart Circ Physiol* 261: H1231–H1245, 1991.
53. **Shoemaker JK, Herr MD, Sinoway LI.** Dissociation of muscle sympathetic nerve activity and leg vascular resistance in humans. *Am J Physiol Heart Circ Physiol* 279: H1215–H1219, 2000.
54. **Task Force of the European Society of Cardiology, and the North American Society of Pacing and Electrophysiology.** Heart rate variability: standards of measurement, physiological interpretation, and clinical use. *Circulation* 93: 1043–1065, 1996.
55. **Taylor JA, Eckberg DL.** Fundamental relations between short-term RR interval and arterial pressure oscillations in humans. *Circulation* 93: 1527–1532.
56. **Taylor JA, Williams TD, Seals DR, Davy KP.** Low-frequency arterial pressure fluctuations do not reflect sympathetic outflow: gender and age differences. *Am J Physiol Heart Circ Physiol* 274: H1194–H1201, 1998.
57. **Tiecks FP, Lam AM, Aaslid R, Newell DW.** Comparison of static and dynamic cerebral autoregulation measurements. *Stroke* 26: 1014–1019, 1995.
58. **Wittmann U, Nafz B, Ehmke H, Kirchheim HR, Persson PB.** Frequency domain of renal autoregulation in the conscious dog. *Am J Physiol Renal Fluid Electrolyte Physiol* 269: F317–F322, 1995.
59. **Zhang R, Zuckerman JH, Giller CA, Levine BD.** Transfer function analysis of dynamic cerebral autoregulation in humans. *Am J Physiol Heart Circ Physiol* 274: H233–H241, 1998.